Nonlinear Wavelet Transforms for Image Coding via Lifting

Roger L. Claypoole, Jr.[†]   Geoffrey M. Davis[‡]

Wim Sweldens[◇]   **Corresponding Author: Richard G. Baraniuk**[† *]

[†] Department of Electrical and Computer Engineering
Rice University, 6100 South Main Street, Houston, TX 77005–1892
clayporl@rice.edu, richb@rice.edu
www.dsp.rice.edu
Phone: (713) 285–5132
Fax: (713) 737–6196

[‡] Microsoft Research, 1 Microsoft Way, Redmond, WA 98052
geoffd@microsoft.com
research.microsoft.com/~geoffd

[◇] Lucent Technologies, Bell Laboratories, 600 Mountain Avenue, Murray Hill, NJ 07974
wim@bell-labs.com

Abstract

We investigate central issues such as invertibility, stability, synchronization, and frequency characteristics for non-linear wavelet transforms built using the lifting framework. The non-linearity comes from adaptively choosing between a class of linear predictors within the lifting framework. We also describe how earlier families of non-linear filter banks can be extended through the use of prediction functions operating on a causal neighborhood of pixels. Preliminary compression results for model and real-world images demonstrate the promise of our techniques.

Permission to publish this abstract separately is granted.

---

1 Introduction

In his classic treatise on the workings of the human visual system, Marr focused on the importance of the *representation* of information for various cognitive tasks [1]. The way in which information is represented brings out certain types of features while hiding others. Image compression applications also rely heavily on having an efficient representation of image data. Ideally we would like to approximate an image with a small number of parameters; the wavelet transform provides such an efficient representation [2].

Transform coding consists of three components: a reversible, linear transform to map the image into a set of transform coefficients; non-reversible quantizers; and an encoder [3, 4]. Typically, a significant number of the transform coefficients are small, and can therefore be coarsely quantized or completely discarded, with little distortion. Compression is achieved during the quantization and encoding of the transformed coefficients, and not during the transformation step.

In this paper we focus on improving the properties of the transform rather than the encoder, expanding on our work in [5]. More precisely, we will construct adaptive wavelet transforms that result in fewer large wavelet coefficients. Such non-linear wavelet transforms provide added flexibility for image representations.

Until recently, the wavelet transforms used for image compression were constructed with linear filter banks. Construction of non-linear filter banks was proposed in [6, 7]. The experiments with a non-linear filter bank for image coding presented in [8] are promising. The key open question in the use of these non-linear constructions is one of design: what is the most effective way to utilize the additional degrees of freedom obtained from relaxing the constraint of linearity?

We examine issues such as invertibility, stability, artifacts, and frequency-domain characteristics (to the extent to which these are well-defined) in the construction of non-linear wavelet transforms. Our analysis builds on the new perspective provided by the lifting framework [9, 10] for the wavelet transform. The lifting framework allows us to incorporate non-linearities while retaining control over the properties of the wavelet transform. The non-linearity comes from adaptively choosing from a set of linear predictors. We also show how the family of non-linear filter banks of [6, 7] can be extended through the use of prediction functions operating on a causal neighborhood.

Our paper is organized as follows. In Section 2, we review the wavelet transform and the lifting construction, and show how to introduce adaptivity into the transform. In Section 3, we discuss issues surrounding adaptivity, and in Section 4 we propose an edge-avoiding adaptive transform. In Section 5, we demonstrate

this transform via compression of artificial and real-world images. We conclude in Section 6 and propose ideas for future research.

2   Wavelets and The Lifting Scheme

2.1   Wavelets

The discrete wavelet transform represents a signal in terms of shifts and dilations of a low-pass scaling function $\phi(t)$ and a bandpass wavelet function $\psi(t)$ [2]. The transform is multiscale, in that it creates a set of coarse coefficients that represent signal information at the lowest scale, and sets of detail coefficients with increasingly finer resolution. The transform is typically implemented as a filter bank with analysis low-pass filter $H(z)$ and high-pass filter $G(z)$, as shown in Figure 1. The inverse transform uses synthesis low-pass $\widetilde{H}(z)$ and high-pass $\widetilde{G}(z)$, as shown in Figure 2. For special choices of H, G, $\widetilde{H}$, and $\widetilde{G}$, the underlying wavelets and scaling functions form a biorthogonal basis and provide perfect reconstruction [2]. The transform is typically iterated on the output of the low-pass band ($c[n]$) to create the series of detail coefficients at different scales.
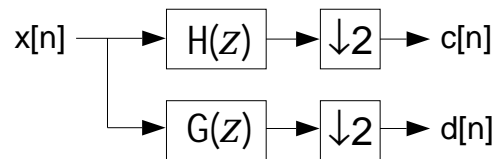

Figure 1: *Filter bank implementation of the wavelet transform. H and G are the analysis low-pass/high-pass pair. $c[n]$ and $d[n]$ are the scaling and wavelet coefficients, respectively.*
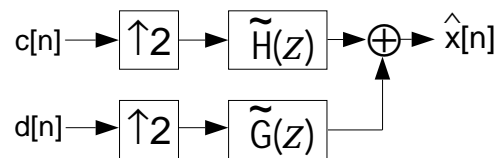

Figure 2: *Filter bank implementation of the inverse wavelet transform. With appropriate choices of $\widetilde{H}$ and $\widetilde{G}$, the transform will yield a perfectly reconstructed output sequence.*

The wavelet representation is efficient because images are often well modeled as a set of locally smooth

regions separated by edges. Within these smooth regions, fine-scale wavelet coefficients are small, and coefficients decay rapidly from coarse to fine scales. In the neighborhood of edges wavelet coefficients decay much more slowly, but because of the local support relatively few wavelet coefficients are affected by edges. However, these large wavelet coefficients near edges are expensive to code. Many image coders are designed to operate on wavelet transformed data, and much current research focuses on enabling these coders to exploit the structure present in wavelet coefficients along edges. Current successful coders perform some form of conditioning [11], variance prediction [12], or context-based entropy coding [13].
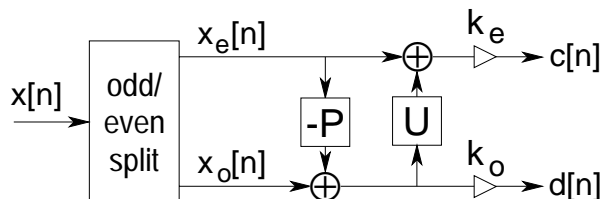
2.2 The Lifting Scheme

Figure 3: *Typical Lifting Steps: Split, Predict, and Update.*

Lifting [9, 10] was originally developed to adjust wavelet transforms to complex geometries and irregular sampling leading to so-called *second generation wavelets*. It can also be seen as an alternate implementation of classical, first generation wavelet transforms [9, 14]. The main feature of lifting is that it provides an entirely spatial-domain interpretation of the transform, as opposed to the more traditional frequency-domain based constructions. The local spatial interpretation enables us to adapt the transform not only to the underlying geometry but also to the data, thereby introducing non-linearities while retaining control of the transform's multi-scale properties.

A typical lifting stage is comprised of three steps: Split, Predict, and Update (as shown in Figure 3):[1]

Split: Let $x[n]$ be a signal. We first *split* $x[n]$ into its even and odd polyphase components $x_e[n]$ and $x_o[n]$, where $x_e[n] = x[2n]$ and $x_o[n] = x[2n+1]$. In this paper we work only with the even and odd polyphase components of $x[n]$, but in principle any partition of $x[n]$ into non-overlapping sets is possible [10]. If the

---

[1]In Figure 3, the outputs of the lifting stage are weighted by k_e and k_o. These values serve to normalize the energy of the underlying scaling and wavelet functions, respectively. Thus, this normalization could be considered a fourth lifting step.

3

$x[n]$ correspond to the samples of an underlying smooth, slowly varying function, then the even and odd polyphase components are highly correlated. This correlation structure is typically local, and thus we should be able to accurately predict each odd polyphase coefficient from the nearby even polyphase coefficients.

Predict: In the interpolating formulation of lifting, we *predict* the odd polyphase coefficients $x_o[n]$ from the neighboring even coefficients $x_e[n]$. The predictor for each $x_o[n]$ is a linear combination of neighboring even coefficients:

$$P(x_e)[n] = \sum_l p_l\, x_e[n+l].\tag{1}$$

We obtain a new representation of the $x[n]$ by replacing $x_o[n]$ with the prediction residual. This leads to the first lifting step:

$$d[n] = x_o[n] - P(x_e)[n].\tag{2}$$

If the underlying signal is locally smooth, the prediction residuals $d[n]$ will be small. Furthermore, the new representation contains the same information as the original signal $x[n]$: given the even polyphase $x_e[n]$ and the prediction residuals $d[n]$, we can recover the odd polyphase coefficients $x_o[n]$ by noting that

$$x_o[n] = d[n] + P(x_e)[n].\tag{3}$$

This prediction procedure is equivalent to applying a high-pass filter to $x[n]$. The prediction filter is typically designed to exactly predict local polynomials up to and including degree $N-1$. In wavelet terminology, the underlying synthesis scaling function corresponding to this prediction filter can reproduce polynomials of degree up to $N-1$, and the dual (analysis) wavelet has N zero moments.

Update: The third lifting step transforms the even polyphase coefficients $x_e[n]$ into a low-pass filtered and subsampled version of $x[n]$. We obtain this coarse approximation by *updating* $x_e[n]$ with a linear combination of the prediction residuals $d[n]$. We replace $x_e[n]$ with

$$c[n] = x_e[n] + U(d)[n],\tag{4}$$

where $U(d)$ is a linear combination of neighboring d values:

$$U(d)[n] = \sum_l u_l\, d[n+l].\tag{5}$$

4

Each lifting step is always invertible; no information is lost. Assuming the same P and U are chosen for the analysis and synthesis stages, the lifting construction guarantees perfect reconstruction for any P and U. Given $d[n]$ and $c[n]$, we have

$$x_e[n] = c[n] - U(d)[n] \tag{6}$$

and $x_o[n]$ from (3).

The inverse lifting stage is shown in Figure 4. Note that c and d are at half rate, and thus this transform corresponds to a critically sampled perfect reconstruction filter bank. One can show that the update function determines the properties of the dual wavelet and primal scaling function. In particular, if the update filter is one-half the adjoint of the predict filter, then the primal (synthesis) wavelet has N zero moments as well [9].
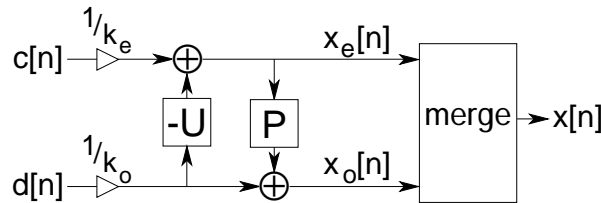

Figure 4: *Typical inverse lifting steps: undo the update, undo the predict, and merge.*

2.3   Examples

A simple example of lifting is the construction of the Deslauriers-Dubuc family of wavelets [9] from a single Deslauriers-Dubuc [15] prediction step followed by a single update step. For example, the following prediction and update steps comprise a single stage of the (4,4) Deslauriers-Dubuc wavelet transform:

$$d[n] = x_o[n] - \left(-x_e[n-1] + 9x_e[n] + 9x_e[n+1] - x_e[n+2]\right)/16\,, \tag{7}$$

$$c[n] = x_e[n] + \left(-d[n-2] + 9d[n-1] + 9d[n] - d[n+1]\right)/32. \tag{8}$$

The predict step cancels cubic polynomials and leaves the residual in the high-pass signal $d[n]$. The update step results in a low-pass and subsampled version of $x[n]$ being placed in $c[n]$. It should be emphasized that lifting is a general construction and not limited to the Deslauriers-Dubuc family. Using the Euclidean algorithm, we can decompose any FIR wavelet transform into a sequence of prediction and update steps [14]. Thus, the lifting implementation shown in Figure 3, with possibly multiple stages, is equivalent to the

filter bank implementation of the wavelet transform shown in Figure 1. Unfortunately at this point we do not have a spatial interpretation for general transforms factored into lifting steps; consequently we currently do not know how to make adaptive versions of general wavelet transforms.

A second example of a non-linear lifting construction is the integer-to-integer S+P transform of Said and Pearlman [16], shown in Figure 5. The outputs $h[n]$ and $c[n]$ of the S algorithm are computed as:

$$h[n] \quad = \quad x_o[n] - x_e[n] \tag{9}$$

$$c[n] \quad = \quad x_e[n] + Q\left(h[n]/2\right) \tag{10}$$

where Q is a round-off operator to ensure the transform is integer-to-integer. The P transform creates the detail coefficients $d[n]$ as:

$$d[n] = h[n] - Q\left(P(c[n]) + P_b(h[n])\right). \tag{11}$$

P_b must be causal to ensure that the inverse transform can be implemented with identical filters to the forward transform.
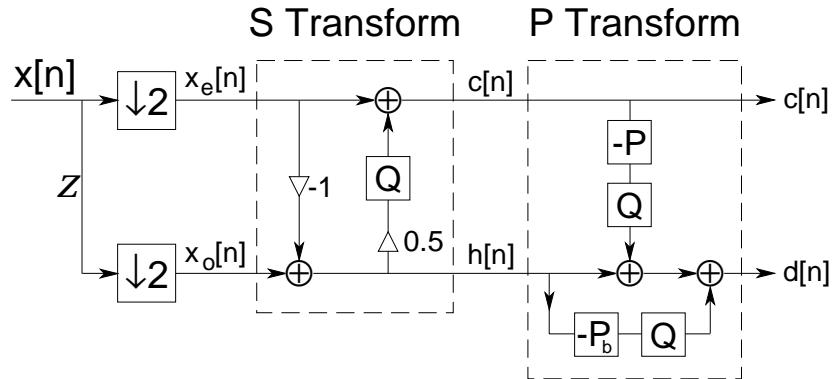

Figure 5: *Said and Pearlman (S+P) transform [16].*

In [17], it was shown that the S+P transform can be seen as a three-step non-linear lifted transform. The S transform is constructed as a one point predict followed by a one point update. The P transform is an additional prediction step, combined with the causal P_b filter. The non-linearity comes from the quantizers which are needed to ensure an integer-to-integer transform. Due to the nature of the lifting implementation (and the causality of P_b), perfect reconstruction is guaranteed despite the presence of the non-linear quantizers. It is interesting to note that the optimized coefficients of the P transform proposed in [16] satisfy some of the linear lifting constraints discussed in Section 2.2.

2.4 Introducing Adaptivity into the Wavelet Transform

Wavelet bases typically employed for image compression (such as the Daubechies (7,9) system [2]) utilize smooth scaling and wavelet functions. Such bases can be easily constructed with the predict-then-update form of lifting described above. Larger predictors (predictors that can exactly predict polynomials of higher degree) correspond to smoother basis functions; these lifting predictors work well when the underlying signal is smooth (just as the Daubechies (7,9) system works best when the signal is smooth).

However, most images consist of regions of smoothness and texture separated by discontinuities (edges). These discontinuities cannot be well-represented by smooth basis functions. Since smooth basis functions correspond to lifting predictors with wide support, these predictors work poorly near edges, when the discontinuity is within the data we are using for the prediction.

Our goal is to *introduce a mechanism that allows us to choose the prediction operator based on the local properties of the image*. This makes the P operator data-dependent and thus non-linear. However, lifting guarantees that the transform remains reversible. In regions where the image is locally smooth, we use higher order predictors. Near edges we reduce the order and thus the length of the predictor. This avoids making a prediction based on data which is separated from the point of interest by a discontinuity. Ideally we would like to use predictors that take into account the fact that discontinuities in images tend to occur along continuous curves. Such an adaptation would allow us to exploit the additional spatial structure that we know exists in edges.

3 Filter Design

Adapting the predictor makes our transform non-linear. However, the concept of basis functions relies fundamentally on linear superposition. Consequently, the notion of a single basis function no longer makes sense for non-linear transforms. We thus focus on the spatial properties of the transform when designing our predictors.

3.1 Multi-resolution Properties

When the prediction and update operators are constructed via the polynomial lifting constraints, the output of the update step is a coarse approximation (low-pass and downsampled) version of our image. We need this coherent interpretation of the update coefficients, since they will be input to further iterations of the

transform. After the first iteration, all subsequent predictions are based on updated coefficients. If we are to make effective prediction throughout the transform, we need some kind of structure in the update. However, if the prediction is performed with a non-linear operator, it may not be possible to construct an update operator that satisfies the polynomial lifting constraints and provides a low-pass interpretation of the updated coefficients.

Consider again the example (8). While it is easy to see that the prediction filter P leads to a high-pass filter, it is not immediately clear that the update U leads to a low-pass filter. The reason is that the lifting structure mandates that the high-pass coefficients d must be reused in the computation of c, and thus c depends both on P and on U. By carefully adjusting the update U to the prediction P, we can ensure that c is a low-pass-filtered and subsampled version of the original signal. In the example, $U(d)$ had to be chosen as $(d[n-2] + 9d[n-1] + 9d[n] + d[n+1])/32$. While we know how to adjust U for a spatially varying, but linear P [10], it is not immediately clear how to construct a non-linear U that preserves frequency localization (to the extent that this is well-defined) when we have a non-linear P.

3.2   Stability and Synchronization

We also need to ensure that the transform is stable. Lossy coding schemes introduce errors into the transform coefficients, so it is crucial that the non-linearities do not unduly amplify these errors. Our goal is to use a high-order predictor in smooth regions and a low-order predictor near edges. In order to avoid sending side information on which predictor was chosen, we need to base the choice only on the $x[n]$. However, in lossy compression the decoder only has the quantized even coefficients $\widehat{x}_e[n]$ rather than the original coefficients $x_e[n]$. If we use locally adapted filters, then quantization errors in coarse scales could cascade across scale and cause a series of incorrect filter choices leading to serious reconstruction errors.

In the predict-then-update case, the problem of stability cannot be solved by synchronization alone, i.e., having the encoder make its choice of predictor based on quantized data. The reason is that the reconstructed values $\widehat{x}_e[n]$ are obtained from quantized low-pass values $\widehat{c}[n]$. The low-pass signal $c[n]$ is a function of the prediction residual signal $d[n]$, which in turn depends on what filters are chosen for prediction, as shown on the left in Figure 6. Hence the encoder cannot obtain the quantized values $\widehat{x}_e[n]$ until it selects a predictor, and it cannot select a predictor without obtaining $\widehat{x}_e[n]$. If we are to employ a non-linear lifting procedure for lossy coding, it is essential that we avoid this Catch 22.
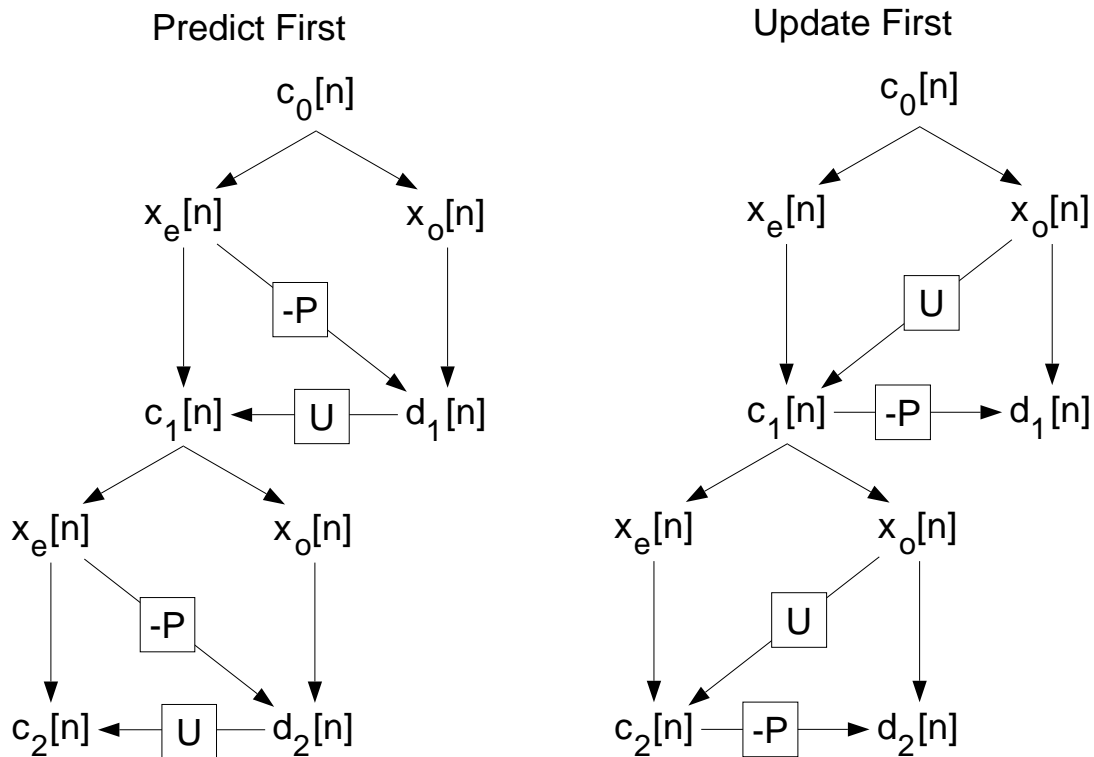
Figure 6: *Two-iteration lifted wavelet transform trees with predict-first (left) and update-first (right). When predicting first, the prediction must be performed prior to construction of the coarse coefficients and iteration to the next scale. When updating first, the prediction operator is outside the loop. The coarse coefficients can be iterated to the lowest scale, quantized, and reconstructed prior to the predictions.*

3.3 Solution: Update First

We propose a simple modification that solves the stability and synchronization problems: reverse the order of the predict and update lifting steps in the wavelet transform (see Figure 7). We first update the even samples based on the odd samples yielding the low-pass coefficients $c[n]$. We then reuse these low-pass coefficients to predict the odd samples, which gives the high-pass coefficients $d[n]$. We use a linear update filter and let only the choice of predictor depend on the data.
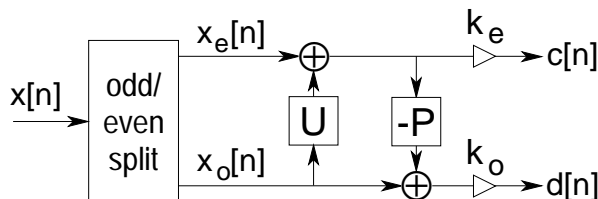

Figure 7: *Update-First Lifting Sequence.*

Because we update first and the transform is only iterated on the low pass coefficients $c[n]$, all $c[n]$ throughout the entire pyramid linearly depend on the data and are not affected by the non-linear predictor. This is shown in Figure 6. The tree on the left shows the predict first pyramid. Clearly, it is impossible to create the coarse coefficients without first using the prediction operator to create the detail coefficients. However, in the update-first tree on the right, the prediction operators are not in the loop. Thus the prediction is only based on low-pass coefficients that are computed as in the classical wavelet transform. Furthermore, if we perform the transform *backwards*, i.e., starting the prediction process at the lowest frequency (coarsest) subband and working from coarse to fine scales, we can keep the encoder and decoder perfectly synchronized. The predictor operates on raw data, but the *choice of predictor* is based on quantized data. This ensures that the encoder and decoder are choosing predictors based on the same data, and eliminates propagation of error due to incorrect decisions at the decoder. Moreover the low-pass branches of our entire multi-resolution scheme now are linear. Consequently we still have the notion of a dual (analysis) scaling function.

Our update-then-predict lifting scheme is related to the Laplacian pyramid of Burt and Adelson [18], in which images are represented as a series of prediction residuals, and the predictors are not constrained to being linear. The Laplacian pyramid has the disadvantage that it expands the number of coefficients in the image being transformed by a factor of $4/3$. Lifting, on the other hand, guarantees a critically sampled

decomposition.

Our implementation is also similar to the framework developed independently by Gerek and Cetin in [19]. However, by constructing our transform via the lifting framework, we are able to incorporate adaptivity while retaining control over the underlying properties of the transform.

4 Adaptive Wavelet Transform

We now have a framework for introducing adaptivity into the wavelet transform. We will create and quantize all the coarse coefficients to the lowest scale (update first), and then adapt the prediction operator P to these coefficients. The question remains on how to determine the appropriate P.

4.1 Edge-Avoiding Prediction

As stated in Section 2.4, our goal is to choose the prediction operator based on the local properties of the image. For each prediction window, we analyze the data to determine if it is well approximated by a low order polynomial. If it is, then we use a high-order predictor with wide support, which corresponds to a smooth basis function. If the data does not meet our smoothness criteria, we determine which pixels in the prediction window contribute to the failure. We classify these pixels as "edge" or discontinuity coefficients. Near these edges we reduce the order of the predictor so that the neighborhood we use for prediction never overlaps the edge. In this manner we maintain high accuracy away from edges, and avoid large errors in the presence of edges. Figure 8 illustrates the process of selecting these predictors near an ideal step edge.
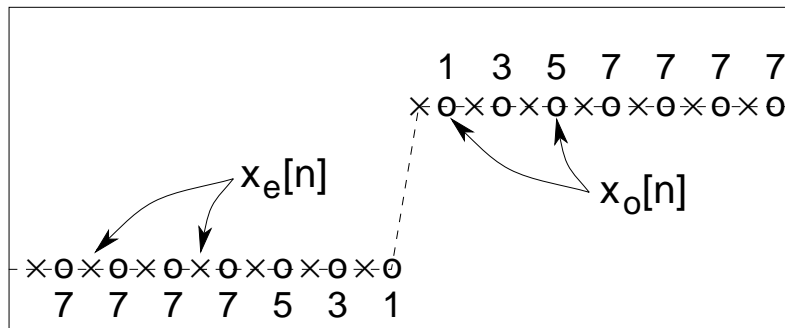

Figure 8: *Predictor selection at an ideal step edge. Numbers indicate the order of the predictors used. The closer to the edge, the lower the order of the predictor.*

4.2 Choice of Prediction Filters

The question remains on how to find the P and U filters even in the linear case. One choice is the same P and U filters from the Deslauriers-Dubuc family, except use P for the update, followed by U for the prediction (with appropriate normalization). Swapping P and U in this fashion reverses the roles of the analysis and synthesis functions. However, this is problematic for coding applications, because the analysis wavelets in the Deslauriers-Dubuc family are much less smooth than the synthesis wavelets [2]. Since reconstructed images are built up from synthesis wavelets, these non-smooth building blocks lead to highly visible artifacts in the reconstructed image when the coefficients are quantized.

It is possible to boost the smoothness of the new building blocks by increasing the size of the filters (and adding more vanishing moments to the underlying scaling and wavelet functions). However, due to the biorthogonal structure of the update-first, single-stage lifting construction, the size of the synthesis filter $\widetilde{H}(z)$ will always be larger that of the analysis filter $H(z)$. We observe that this leads to excessive ripple in the new building blocks, which in turn causes ringing in our reconstructed image.

Instead we propose a solution based on Donoho's average-interpolation that fits into the update-predict form of lifting [20, 21]. This leads to the $(1, N)$ branch of the Cohen-Daubechies-Feauveau family which is biorthogonal to the box function [22]. Let us consider a simple example. The low-pass coefficients are computed using a Haar filter:

$$c[n] = (x[2n] + x[2n + 1])/2. \tag{12}$$

The high-pass coefficients are the residuals of a prediction of the odd samples based on the $c[n]$. The first-order Haar prediction is

$$d[n] = x[2n + 1] - c[n], \tag{13}$$

while the third-order predictor, i.e., one that is exact for quadratics, is given by

$$d[n] = x[2n + 1] - (-c[n - 1]/8 + c[n] + c[n + 1]/8). \tag{14}$$

Predictors of higher order can be built in a straightforward way. The smoothness of the resulting scaling functions increases with the order. A lower bound for the Hölder regularity $R(N)$ as a function of N is given by $R(3) = 0.678$, $R(5) = 1.272$, $R(7) = 1.826$, $R(9) = 2.354$, and asymptotically $R(k) \approx 0.2075N$ [20]. The scaling and wavelet functions for the (1,7) set are shown in Figure 9. In numerical experiments this

filter set yields compression performance approaching that of the Daubechies (7,9) filter set that is more commonly used in image coding applications.

Analysis Scaling Function

Synthesis Scaling Function

Analysis Wavelet Function
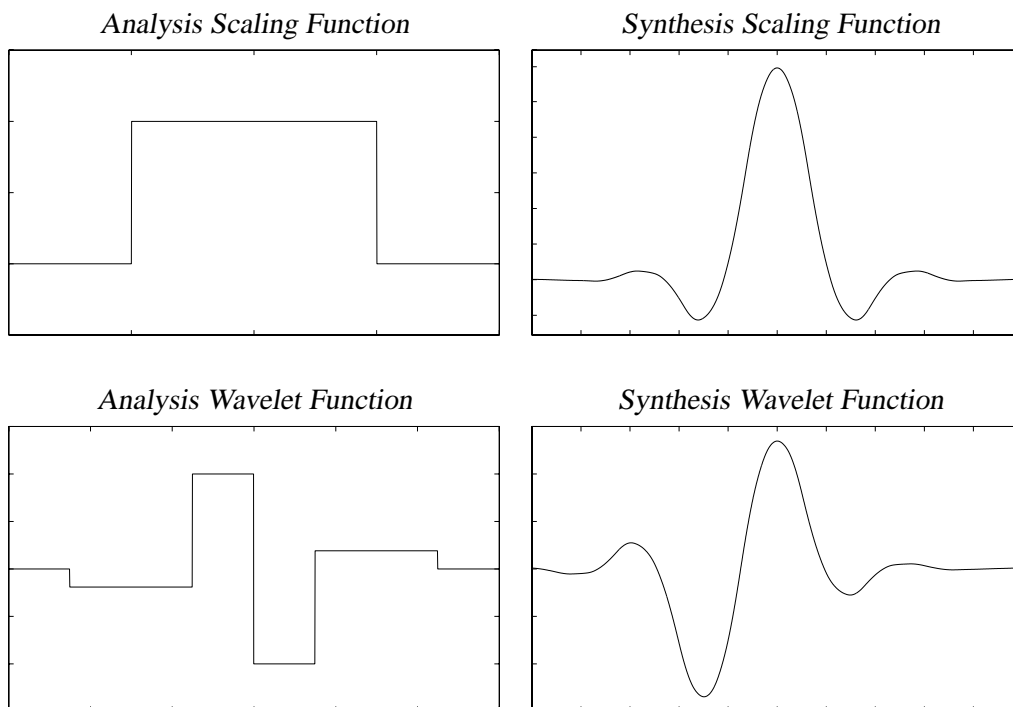
Synthesis Wavelet Function

Figure 9: *Scaling and Wavelet functions for the order (1,7) Cohen-Daubechies-Feauveau filter used in our experiments. These basis functions correspond to the update first form of lifting.*

This non-linear lifting framework generalizes the ideas of de Quieroz *et. al.* [8] and makes clear the relationship between the non-linear filter banks described by these authors and the wavelet transform. The filter bank described in [8] generates the high-pass subbands using a non-separable median filter, and the low-pass subbands via down-sampling. This filter bank performs particularly well for test images containing sharp edges, such as the *cameraman* image and text; it minimizes problems with ringing around the edges. However, the transform suffers from speckling artifacts due to aliasing of high frequency noise into the low-pass subbands. Our use of an anti-aliasing function via lifting has the potential to eliminate this speckling while maintaining high quality reconstruction around edges.

The idea of adaptively choosing from the (1,N) family of filters is similar to the work done independently by Boulgouris et al. [23], who use the (N,2) family (predict first) to provide additional vanishing moments in the synthesis wavelet function for improved *lossless* image compression. However, our update first architecture provides for encoder/decoder synchronization (see Section 4.3, below) despite our application to

lossy compression.

4.3 Synchronization

As we stressed in Section 3.3, maintaining synchronization between the adaptations of the encoder and the decoder is essential for a stable inversion. Encoding a j-level transform proceeds as follows: we first compute the coarsest scale coefficients of the transform $\overset{.}{c}[n]$ by iterating the linear update procedure j times. We quantize $c^j[n]$ to $\widehat{c}^j[n]$ and transmit them. Then we compute the high-pass coefficients $d[n]$ as

$$d[n] = c^{j-1}[2n+1] - P_{\widehat{c}^j}(c^j)[n], \tag{15}$$

quantize them to $\widehat{d}[n]$ and transmit them. Although the predictor operates on the unquantized $\overset{.}{c}[n]$, the *choice* of predictor, $P_{\widehat{c}^j}$, is based on the quantized data $\widehat{c}^j[n]$. Both encoder and decoder now need the quantized values of the next finer scale $\widehat{c}^{j-1}$; the even and odd components are respectively computed by undoing the prediction and update step, but now based on the *quantized* values $\widehat{c}^j[n]$:

$$
\begin{aligned}
\widehat{c}_o^{j-1}[n] &= \widehat{c}^{j-1}[2n+1] = \widehat{d}^j[n] + P_{\widehat{c}^j}(\widehat{c}^j)[n], \\
\widehat{c}_e^{j-1}[n] &= \widehat{c}^{j-1}[2n] = 2\,\widehat{c}^j[n] - \widehat{c}^j[2n+1].
\end{aligned}
\tag{16}
$$

We now can compute the high-pass coefficients on the next finer level. By basing our choice of predictor at each stage on the quantized values $\widehat{c}$, we maintain synchronization between encoder and decoder, and prevent propagation of quantization errors due to incorrect prediction filter choices.

Note that it is possible to use quantized data, not only for determining the prediction filter, but for the actual prediction as well. The lifting construction provides perfect reconstruction despite the presence of this non-linear (quantization) prediction operator. The decoder and encoder will be synchronized not just in the *choice* of prediction filter, but also in the *output* of the prediction filter. However, the quality of this output (accuracy of the prediction) will be highly dependent on the level of quantization. Even for moderately quantized data, our research has shown that prediction errors will tend to be large, regardless of prediction filter. Thus, feeding quantized data into the prediction operator decreases the energy compaction properties of the wavelet transform and reduces the compression potential of our adaptive algorithm.

4.4   2-D Prediction Windows

Since all the quantized coarse coefficients are available to both the encoder and decoder, we can utilize the data above and below the point of interest to determine our choice of predictors. That is, our edge-detection algorithm can analyze the data in this nonseparable 2-D prediction window to determine the location and orientation of the edge. Edges in images are actually contours; they have significant geometric structure. By using a nonseparable 2-D window, we can exploit this edge structure to make smarter prediction decisions within the framework of our separable transform.

If we sense (by our outlier method described earlier) that an edge is present within our prediction window, we analyze the data in the 2-D window around the point of interest to refine our estimate of the edge. We assume a step edge is present, project the data onto a truncated Fourier basis, and qualify our projection against our edge model. This process is a modified version of the algorithm presented in [24]. If the data passes our edge criteria, the intensity and angle of the edge are determined. This information is then used to refine our choice of prediction filter.

non-linear lifting also allows us to use not only the low-pass coefficients for prediction of $x_o[n]$, but also other odd coefficients in a causal neighborhood of $x_o[n]$. Suppose our signal $x[n]$ is a row in an image. We would predict $x_o[n]$ from low-pass coefficients $c[n]$ on its left and right. Further suppose we have discovered a vertical step edge near $x_o[n]$. The precise location of the edge cannot be determined from the low-pass coefficients $c[n]$. However, if we know the value of the coefficients from the row *directly above* $x_o[n]$, we can use this information in the prediction of $x_o[n]$. This predict-from-above idea is similar to the causal P_b filter of the S+P algorithm [16] discussed in Section 2.3.

Predict-from-above offers potential reductions in prediction errors. This increased flexibility comes at the price of decreased stability. Consider the example above in which we resolve difficulties in predicting the location of a vertical edge in a row of coefficients by using already inverted coefficients in the row above. Such a scheme permits a quantization error in one row to propagate along a vertical edge to all other rows. We can prevent such propagation by employing a Differential Pulse Code Modulation (DPCM)-like strategy [25] of using *quantized* data from the causal neighborhood for making predictions in the encoder as well as in the decoder. This strategy will only work in the horizontal direction, since the vertical transform must be completed before the horizontal transform can be computed. Also, the quality of this prediction-from-above will be highly dependent on the level of quantization. Even for moderately quantized data, the prediction

errors will tend to be large, again decreasing the energy compaction and compression potential. Thus, the nonseparable 2-D prediction window leads to a better choice of prediction filters (and better compression), but using the quantized data in this window to perform the actual prediction may not.

5 Results

5.1 Synthetic Data

Figure 10 shows the result of our adaptive lifting algorithm applied to an edge-dominated test image. This image was constructed by superimposing texture on shapes of different magnitudes and orientations. The original image was transformed and compressed to 0.67 bits-per-pixel (BPP) (12:1 compression) using an embedded zero-tree encoder [26]. For simplicity, we compress the zero-tree symbol stream with a Huffman coder, and we make no effort to compress the quantization bit stream.

We notice that the Daubechies (7,9) and linear (1,7) lift transformed images suffer from blurring and ringing around the edges. However, the image transformed with our adaptive lifted algorithm has much sharper edges. Ringing is reduced, edge sharpness is maintained, and the background texture is not significantly corrupted. These improvements are very visible in the closeup shown in Figure 11. The reason for these improvements is that edges in our new transform are represented in a more compact fashion, and as a result there is less degradation of the image when we zero out small, non-zero coefficients.

As a performance metric, we compute the peak signal to noise ratio (PSNR),

$$\text{PSNR} = 20 \log \left(\frac{\max(x_i)}{\sqrt{\sum (x_i - \widehat{x}_i)^2 / N}} \right),$$

where x_i is the ith pixel or our original image, $\widehat{x}_i$ is the ith pixel or our reconstructed image, and N is the total number of pixels. The PSNR curve (Figure 12) demonstrates that, for this edge-dominated test image, the adaptive algorithm has better PSNR performance than both the Daubechies (7,9) and linear (1,7) lift transforms. The Daubechies (7,9) PSNR curve is shown for reference only; our goal is to improve the performance of the linear (1,7) lift though adaptivity.

5.2 Real Data

In Figure 13, we see the result of our adaptive lifting algorithm on the image *cameraman*, compressed to 0.32 BPP (25:1 compression). Our prediction decisions are based on data quantized to 7 iterations of the

Original Image

Compressed with Daubechies (7,9)

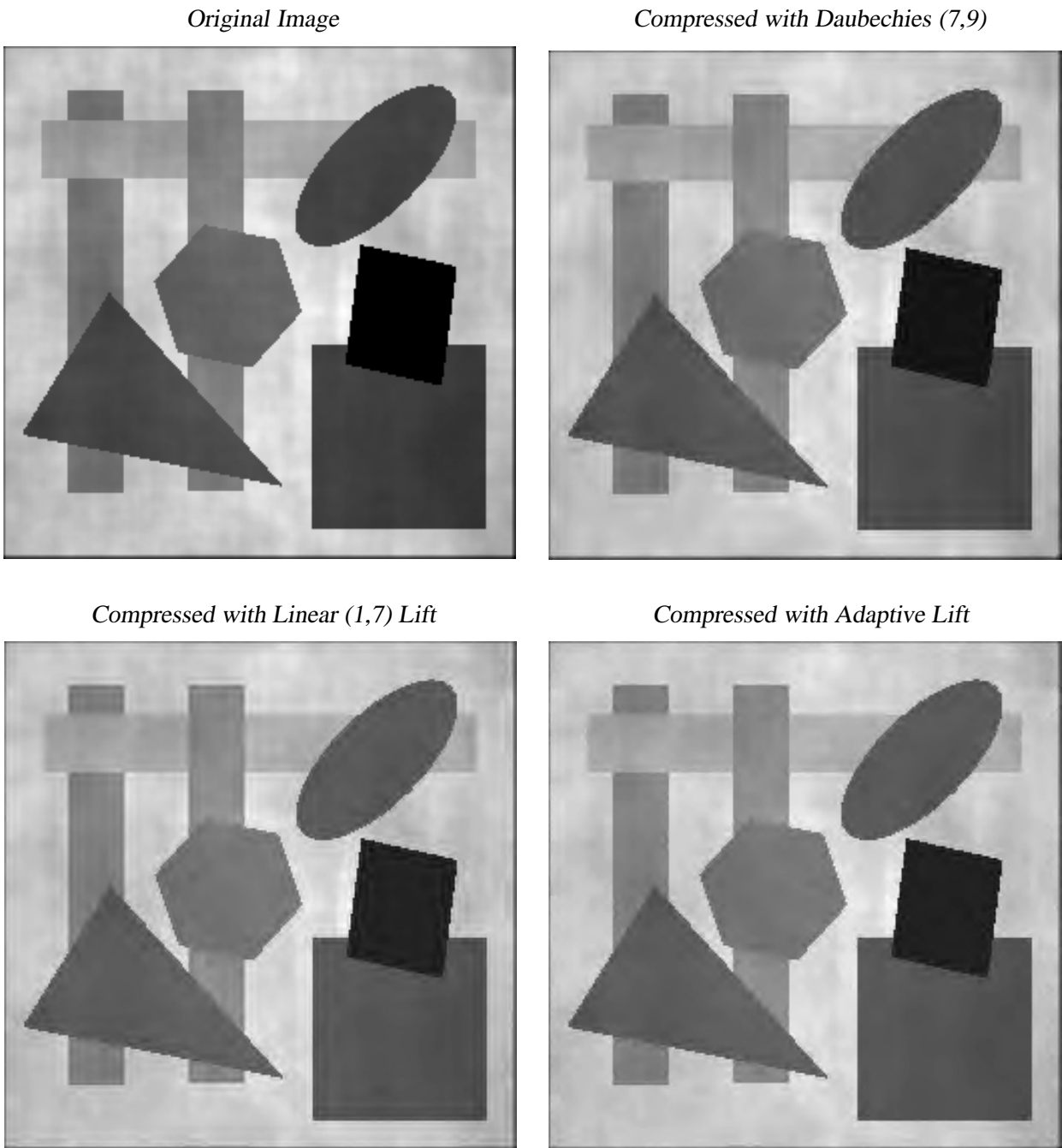*Compressed with Linear (1,7) Lift*

Compressed with Adaptive Lift

Figure 10: *Edge dominated image with texture, compressed to 0.67 BPP (12:1 compression). Note the ringing around the edges of the square in the Daubechies (7,9) and linear (1,7) lift images that is eliminated by the adaptive lift.*
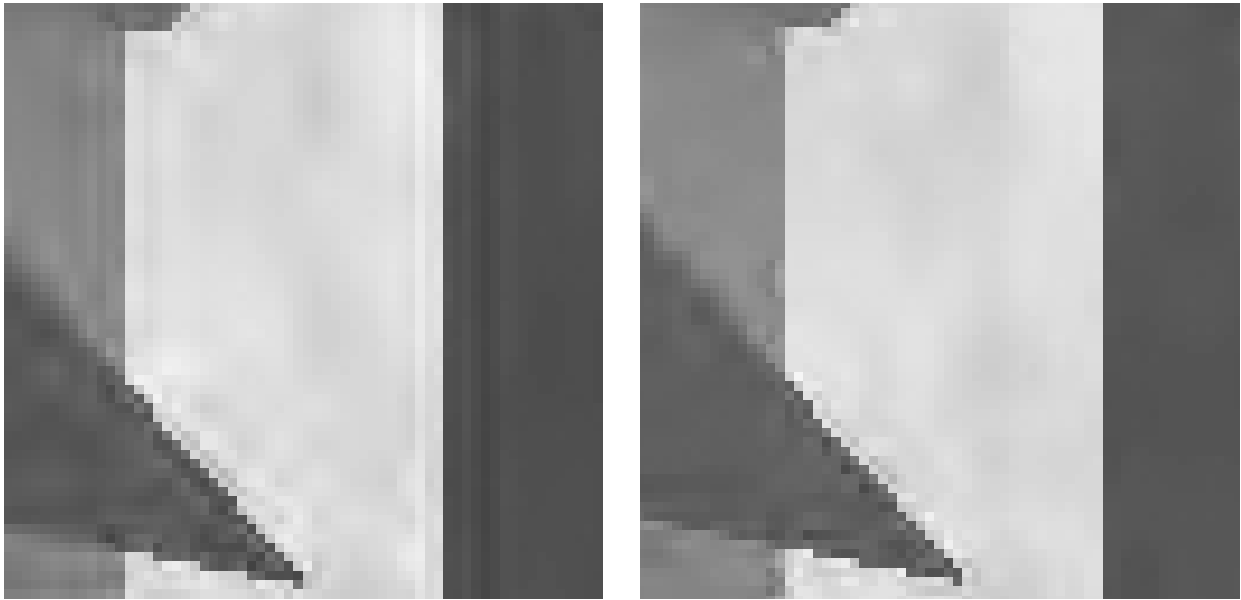
Figure 11: *Close-up of edge dominated image with texture, compressed to 0.67 Bits-Per-Pixel (BPP) (12:1 compression). Note the sharp edges and reduced ringing with the adaptive algorithm.*

zero-tree encoder to ensure that the decoder/encoder synchronization. While ringing has been reduced in the horizontal and vertical edges, there are still some ringing artifacts in the diagonal direction. The reason for these remaining artifacts is that we are using a separable transform in which we seek to avoid horizontal and vertical edges.

Note in Figure 14 the PSNR performance of our adaptive algorithm over the linear (1,7) lift. Each point on the PSNR curve was generated with decoder/encoder synchronization. Again, the performance of the popular Daubechies (7,9) transform is shown for reference. Although our adaptive algorithm does not match the PSNR performance of the Daubechies (7,9) transform, the visual quality of our algorithm is comparable, due to the reduction in edge artifacts. In general the adaptive algorithm results in much sharper decoded images. We conjecture that introducing adaptivity into the Daubechies (7,9) transform (an area of current research) would result in further PSNR increases.
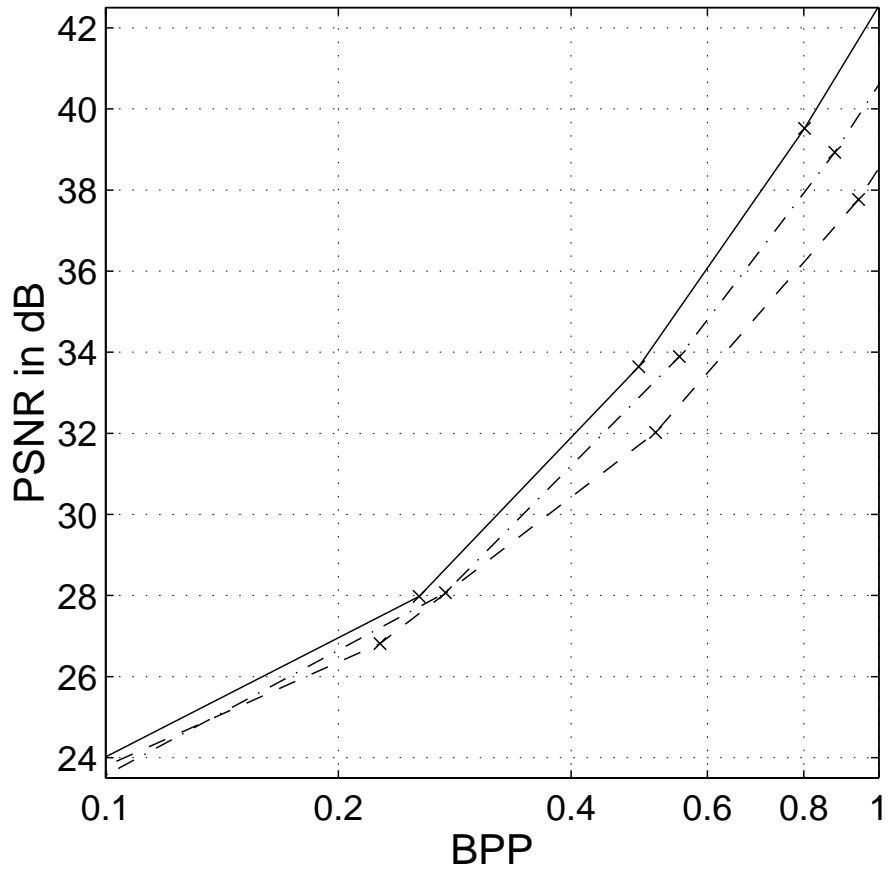
Figure 12: *Peak Signal-to-Noise Ratio (PSNR) curves for the edge-dominated test image of Figure 10. This test image was designed to demonstrate the potential gains of the adaptive lift. The adaptive algorithm (solid line) outperforms the Daubechies (7,9) transform (dash-dot) and the (1,7) linear lift (dash). The encoder and decoder were synchronized for the adaptive algorithm.*

Cameraman Image

Compressed with Daubechies (7,9)

Compressed with Linear (1,7) Lift

Compressed with Adaptive Lift

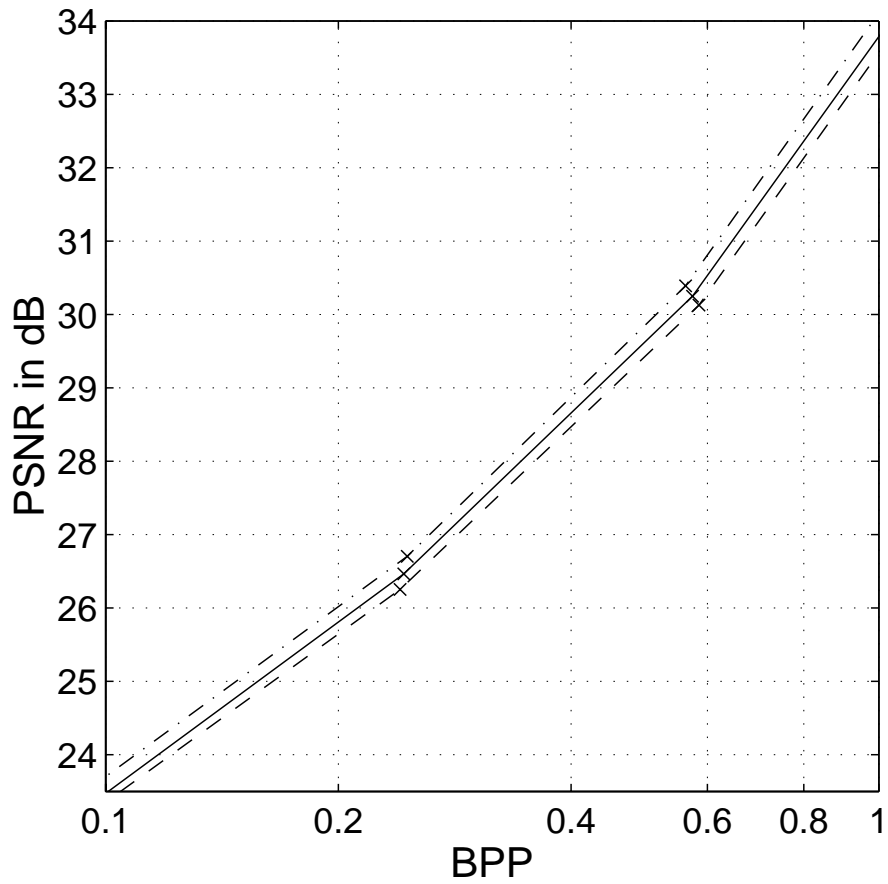Figure 13: *Cameraman image compressed to 0.32 BPP (25:1 compression).*

Figure 14: *PSNR curves for the cameraman image. The adaptive algorithm (solid line) outperforms its linear (1,7) lift (dash), but it does not meet the PSNR performance of the Daubechies (7,9) transform (dash-dot). However, edge artifacts are significantly reduced by the adaptive algorithm. The encoder and decoder were synchronized for the adaptive algorithm.*

6 Conclusions

Lifting provides insight into the construction of the wavelet transform, and allows us to incorporate adaptivity and non-linear operators into the transform. We presented the *Update First* scheme to maintain control over the multi-resolution properties of the transform despite the presence of these non-linearities.

Within this scheme, we introduced an algorithm that switches between various linear predictors to *avoid predicting across edges*. This algorithm efficiently represents edges and compacts energy into the lower subbands of the transform. In addition, we employed a *2-D non-separable window* to make better predictor choices and to improve the quality of the prediction itself. The update-first scheme allowed us to make these improvements while maintaining synchronization between the encoder and decoder (to prevent propagation of quantization errors).

Our adaptive lifting transform appears promising for lossy compression. It reduces edge artifacts and ringing, and improves PSNR performance on certain test images.

Thus, the lifting scheme permits us to combine the best of both worlds. We can introduce non-linear and adaptive filters into our transform, while simultaneously maintaining the multi-resolution properties of the linear wavelet transform. This provides a very powerful tool for not only lossy image compression, but other applications as well, such as lossless image compression [23], image estimation [27], image classification, and feature extraction.

References

[1] David Marr, *Vision*, W. H. Freeman, New York, 1982.

[2] I. Daubechies, *Ten Lectures on Wavelets*, CBMS-NSF Regional Conf. Series in Appl. Math., Vol. 61. Society for Industrial and Applied Mathematics, Philadelphia, PA, 1992.

[3] R. J. Clark, *Transform Coding of Images*, Academic Press, New York, NY, 1985.

[4] R. Gonzalez and R. Woods, *Digital Image Processing*, Addison-Wesley, Reading, MA, 1992.

[5] R. Claypoole, G. Davis, W. Sweldens, and R. Baraniuk, "Nonlinear wavelet transforms for image coding," in *Proc. of Asilomar Conf. on Signals, Systems and Computers*, Nov. 1997.

[6] Dinei A. F. Florêncio and Ronald W. Schafer, "Perfect reconstructing nonlinear filter banks," in *Proc. IEEE Int. Conf. Acoust., Speech, and Signal Proc.*, 1996.

[7] F. J. Hampson and J.-C. Pesquet, "A nonlinear subband decomposition with perfect reconstruction," in *Proc. IEEE Int. Conf. Acoust., Speech, and Signal Proc.*, 1996.

[8] R. de Quieroz, D. A. F. Florêncio, and R. W. Schafer, "Non-expansive pyramid for image coding using a non-linear filter bank," *IEEE Trans. Image Processing*, 1996, Preprint.

[9] W. Sweldens, "The lifting scheme: A custom-design construction of biorthogonal wavelets," *Appl. Comput. Harmon. Anal.*, vol. 3, no. 2, pp. 186–200, 1996.

[10] W. Sweldens, "The lifting scheme: A construction of second generation wavelets," *SIAM J. Math. Anal.*, vol. 29, no. 2, pp. 511–546, 1997.

[11] Eero Simoncelli, "Statistical models for images: compression, enhancement and synthesis," in *Proc. of Asilomar Conf. on Signals, Systems and Computers*. IEEE Signal Processing Society, Nov. 1997.

[12] K. Ramchandran S. LoPresto and M. Orchard, "Image coding based on mixture modeling of wavelet coefficients and a fast estimation-quantization framework," in *Proc. Data Compression Conference*, Snowbird, Utah, Mar. 1997.

[13] C. Chrysafis and A. Ortega, "Efficient context-based entropy coding for lossy wavelet image compression," in *Proc. Data Compression Conference*, Mar 1997, pp. 241–250.

[14] I. Daubechies and W. Sweldens, "Factoring wavelet transforms into lifting steps," *J. Fourier Anal. Appl.*, vol. 4, no. 3, pp. 245–267, 1998.

[15] G. Deslauriers and S. Dubuc, "Symmetric iterative interpolation processes," *Constr. Approx.*, vol. 5, no. 1, pp. 49–68, 1989.

[16] A. Said and W. A. Pearlman, "An image multiresolution representation for lossless and lossy image compression," *IEEE Trans. Image Process.*, vol. 5, no. 9, pp. 1303–1310, 1996.

[17] R. Calderbank, I. Daubechies, W. Sweldens, and B.-L. Yeo, "Wavelet transforms that map integers to integers," *Appl. Comput. Harmon. Anal.*, vol. 5, no. 3, pp. 332–369, 1998.

[18] P. J. Burt and E. H. Adelson, "Laplacian pyramid as a compact image code," *IEEE Trans. Commun.*, vol. 31, no. 4, pp. 532–540, 1983.

[19] Omer Gerek and Enis Cetin, "Linear/nonlinear adaptive polyphase subband decomposition structures for image compression," in *Proc. IEEE Int. Conf. Acoust., Speech, and Signal Proc.*, 1998, vol. 3, pp. 1345–1348.

[20] D. L. Donoho, "Smooth wavelet decompositions with blocky coefficient kernels," in *Recent Advances in Wavelet Analysis*, pp. 259–308. Academic Press, 1993.

[21] W. Sweldens and P. Schröder, "Building your own wavelets at home," in *Wavelets in Computer Graphics*, pp. 15–87. ACM SIGGRAPH Course Notes, 1996.

[22] A. Cohen, I. Daubechies, and J. Feauveau, "Bi-orthogonal bases of compactly supported wavelets," *Comm. Pure Appl. Math.*, vol. 45, pp. 485–560, 1992.

[23] D. Tzovaras N. V. Boulgouris and M. G. Strintzis, "Lossless image compression based on optimal prediction, adaptive lifting and conditional arithmetic coding," *submitted to IEEE Trans. Image Process*, Dec 1998.

[24] K. Jensen and D Anastassiou, "Subpixel edge localization and the interpolation of still images," *IEEE Trans. Image Process.*, vol. 4, no. 3, pp. 285–295, March 1995.

[25] N.S. Jayant and P. Noll, *Digital Coding of Waveforms*, Prentice Hall, Englewood Cliffs, NJ, 1984.

[26] J. M. Shapiro, "Embedded image coding using zerotrees of wavelet coefficients," *IEEE Trans. Signal Process.*, vol. 41, no. 12, pp. 3445–3462, 1993.

[27] R. Claypoole, R. Baraniuk, and R. Nowak, "Adaptive wavelet transforms via lifting," in *Proc. IEEE Int. Conf. Acoust., Speech, and Signal Proc.*, May 1998.